Effects of Macroporous Resin Size on *Candida antarctica* Lipase B Adsorption, Fraction of Active Molecules, and Catalytic Activity for Polyester Synthesis

Bo Chen,[†] Elizabeth M. Miller,[‡] Lisa Miller,[§] John J. Maikner,[‡] and Richard A. Gross*,[†]

NSF I/UCRC for Biocatalysis and Bioprocessing of Macromolecules, Polytechnic University, 6 Metrotech Center, Brooklyn, New York 11201, Rohm and Haas Co., P.O. Box 904, Spring House, Pennsylvania 19477, and National Synchrotron Light Source, Brookhaven National Laboratory, Upton, New York 11973

Received July 31, 2006. In Final Form: October 7, 2006

Methyl methacrylate resins with identical average pore diameter (250 Å) and surface area (500 m^2/g) but with varied particle size (35 to 560−710 μm) were employed to study how immobilization resin particle size influences *Candida antarctica* Lipase B (CALB) loading, fraction of active sites, and catalytic properties for polyester synthesis. CALB adsorbed more rapidly on smaller beads. Saturation occurred in less than 30 s and 48 h for beads with diameters 35 and 560−710 μm, respectively. Linearization of adsorption isotherm data by the Scatchard analysis showed for the 35 μm resin that: (i) CALB loading at saturation was well below that required to form a monolayer and fully cover the support surface and (ii) CALB has a high affinity for this resin surface. Infrared microspectroscopy showed that CALB forms protein loading fronts for resins with particle sizes 560−710 and 120 μm. In contrast, CALB appears evenly distributed throughout 35 μm resins. By titration with *p*-nitrophenyl *n*-hexyl phosphate (MNPHP), the fraction of active CALB molecules adsorbed onto resins was <50% which was not influenced by particle size. The fraction of active CALB molecules on the 35 μm support increased from 30 to 43% as enzyme loading was increased from 0.9 to 5.7% (w/w) leading to increased activity for ϵ-caprolactone (ϵ-CL) ring-opening polymerization. At about 5% w/w CALB loading, by decreasing the immobilization support diameter from 560−710 to 120, 75, and 35 μm, conversion of ϵ-CL % to polyester increased (20 to 36, 42, and 61%, respectively, at 80 min). Similar trends were observed for condensation polymerizations between 1,8-octanediol and adipic acid.

Introduction

Application of immobilized enzymes in biocatalytic practice offers unique advantages over soluble enzymes, such as enhanced activity, increased selectivity, improved stability, and reusability. Adsorption is a simple and straightforward route for biomolecule immobilization. By this method, sufficient quantities of active enzyme have been immobilized and used for industrial processes. For example, Assemblase, the commercial name of immobilized pencillin-G acylase from *Escherichia coli*, has been used by industry for manufacture of the semi-synthetic β-lactam antibiotic cephalexin.[1,2]

Candida antarctica Lipase B (CALB), due to its unique properties, is attracting increased attention as a biocatalyst for the synthesis of low molar mass and polymeric molecules.[3−6] Almost all publications on immobilized CALB use the commercially available catalyst Novozyme 435, which consists of CALB physically adsorbed onto a macroporous acrylic polymer resin (Lewatit VP OC 1600, Bayer). Primarily, commercial uses of CALB are limited to production of high-priced specialty chemicals[7−9] because of the high cost of commercially available CALB preparations: Novozyme 435 (Novozymes A/S) and Chirazyme (Roche Molecular Biochemicals). It is urgent for CALB and other enzymes of commercial importance to focus attention on studies to better correlate enzyme activity to support parameters. The outcome of such work will lead to improved catalysts that have acceptable price-performance characteristics for an expanded range of industrial processes.

Most research on immobilization has focused on choice of matrix materials and optimization of immobilization conditions,[10−21] such as hydrophobicity of the support surface[17−19] and pH[20,21] of the enzyme solution. Physical properties of supports

* Corresponding author. E-mail: rgross@poly.edu.
[†] Polytechnic University.
[‡] Rohm and Haas Co.
[§] Brookhaven National Laboratory.

(1) Schroën, C. G. P. H.; Nierstrasz, V. A.; Moody, H. M.; Hoogschagen, M. J.; Kroon, P. J.; Bosma, R.; Beeftink, H. H.; Janssen, A. E. M.; Tramper, J. *Biotechnol. Bioeng.* **2001**, *73*, 171−178.
(2) Schroën, C. G. P. H.; Nierstrasz, V. A.; Kroon, P. J.; Bosma, R.; Janssen, A. E. M.; Beeftink, H. H.; Tramper, J. *Enzyme Microb. Technol.* **1999**, *24*, 498−506.
(3) Gross, R. A.; Kalra, B. *Science* **2002**, *297*, 803−806.
(4) Gross, R. A.; Kumar, A.; Kalra, B. *Chem. Rev.* **2001**, *101*, 2097−2124.
(5) Kobayashi, S.; Uyama, H.; Kimura, S. *Chem. Rev.* **2001**, *101*, 3793.
(6) Cheng, H. N., Gross, R. A., Eds.; *Polymer Biocatalysis and Biomaterials*; ACS Symposium Series 900; American Chemical Society: Washington, DC, 2005.
(7) Kirk, O.; Christensen, M. W. *Org. Process Res. Dev.* **2002**, *6*, 446−451.
(8) Anderson, E. M.; Larsson, K. M.; Kirk, O. *Biocatal. Biotransform.* **1998**, *16*, 181−204.
(9) Houde, A.; Kademi, A.; Danielle *Appl. Biochem. Biotechnol.* **2004**, *118*, 155−170.
(10) Dyal, A.; Loos, K.; Noto, M.; Chang, S. W.; Spagnoli, C.; Shafi, K. V. P. M.; Ulman, A.; Cowman, M.; Gross, R. A. *J. Am. Chem. Soc.* **2003**, *125*, 1684−1685.
(11) Dessouki, A. M.; Atia, K. S. *Biomacromolecules* **2002**, *3*, 432−437.
(12) Maury, S.; Buisson, P.; Pierre, A. C. *Langmuir* **2001**, *17*, 6443−6446.
(13) Soellner, M. B.; Dickson, K. A.; Nilsson, B. L.; Raines, R. T. *J. Am. Chem. Soc.* **2003**, *125*, 11790−11791.
(14) Duracher, D.; Elaissari, A.; Mallet, F.; Pichot, C. *Langmuir* **2000**, *16*, 9002−9008.
(15) Lei, C.; Shin, Y.; Liu, J.; Ackerman, E. J. *J. Am. Chem. Soc.* **2002**, *124*, 11242−11243.
(16) Gill, I.; Pastor, E.; Ballesteros, A. *J. Am. Chem. Soc.* **1999**, *121*, 9487−9496.
(17) Bastida, A.; Sabuquillo, P.; Armisen, P.; Fernandez-Lafuente, R.; Huguet, J.; Guisan, J. M. *Biotechnol. Bioeng.* **1998**, *58*, 486−493.
(18) Sigal, G. B.; Mrksich, M.; M., G. *J. Am. Chem. Soc.* **1998**, *120*, 3464−3473.
(19) Koutsopoulos, S.; van der Oost, J.; Norde, W. *Langmuir* **2004**, *20*, 6401−6406.
(20) Xu, K.; Klibanov, A. M. *J. Am. Chem. Soc.* **1996**, *118*, 9815−9819.
(21) Pancera, S. M.; Gliemann, H., Schimmel, T.; Petri, D. F. S. *J. Phys. Chem. B* **2006**, *110*, 2674−2680.

10.1021/la062258u CCC: $37.00
Published on Web 12/29/2006

also showed significant influence on enzyme loading and catalytic behavior. For example, loading and the specific activity of penicillin-G acylase increased with decreased particle size.[22] Vertegel and Dordick reported that, relative to larger particles, adsorption of lysozyme onto nanoparticles resulted in less loss of lysozyme α-helicity and higher catalytic activity.[23] CALB, adsorbed onto mesoporous silica, functionalized by octyltriethoxysilane, showed high enzyme loading (200 mg protein/g of silica) and catalytic activity for acylation of ethanolamine with lauric acid.[24] The authors attributed excellent catalytic properties to high porosity and hydrophobic character of the support. CALB, adsorbed on octyl-agarose, was highly enantioselective ($E = 25$) for hydrolysis of the *R*-isomer of chiral *R*,*S*-mandelic acid esters whereas the nonimmobilized enzyme showed much lower enantioselectivity ($E < 2$).[25] Our laboratory physically adsorbed CALB onto commercially available macroporous supports that differed in surface composition, hydrophobicity, pore diameter, and surface area. Higher activity for polyester synthesis was observed for CALB-matrix systems that had (i) increased density of CALB molecules within matrix pores and (ii) CALB distributed throughout the matrix.[26]

Although often overlooked, the distribution of enzyme in carriers is critical to understanding catalyst activity. For example, knowledge that an enzyme is primarily located within outer regions of an immobilization support instead of being uniformly distributed throughout the matrix enables meaningful calculations of enzyme density along matrix surfaces as well as improved predictive models of substrate/product diffusion to and from immobilized protein. Jeroen van Roon et al. quantitatively determined intraparticle enzyme distribution of Assemblase using light microscopy.[27] The matrix was sectioned ,and penicillin-G acylase was labeled with specific antibodies. They reported the enzyme was distributed heterogeneously, and its concentration was radius-dependent. Our laboratory reported the use of infrared microspectroscopy for analysis of protein spatial distribution within macroporous polymer supports.[28] With a synchrotron beam light source, spatial resolutions down to 5 by 5 μm were achieved.[26,28] IR absorbance bands corresponding to CALB and the polymer matrix distinguish these two components and were used to generate semiquantitative maps of protein distribution throughout the matrix.

Relative to small molecules, the effects of mass transfer on conversion and catalytic constants will be greater for macromolecular substrates. Since diffusion of substrates and products to and from the catalyst will be largely determined by the size of macroporous particles, this variable is particularly important when assessing catalytic supports for enzyme-catalyzed polymer synthesis and modification reactions. To our knowledge, no systematic studies have been reported on how size of macroporous resins influences enzyme activity.

In this paper, the effect of matrix particle size on CALB-catalyst properties was studied. CALB was adsorbed on a series of resins composed of poly(methyl methyacrylate) that differ in particle size but have similar surface area and pore size values. CALB adsorption isotherms were measured as a function of resin particle and protein concentration. Catalytic activity of immobilized CALB systems was evaluated by ϵ-caprolactone ring-opening polymerizations and adipic acid/1,8-octanediol polycondensations. The fraction of active CALB was measured by active site titration. In addition, enzyme distribution within supports was determined by infrared microspectroscopy. Differences in enzyme distribution and catalyst properties were observed that will provide a basis to others that seek to design optimal immobilized enzyme catalysts for low molar mass and polymerization reactions.

Experimental Section

Materials. *C. antarctica* Lipase B (CALB) in the form of a spay dried powder was a kind gift of Novozymes (Bagsvaerd, Denmark). The SDS−PAGE analysis of an aqueous solution of this powder showed a single band with a molecular weight (33 K Da) corresponding to CALB. Macroporous poly(methyl methacrylate) resins were kind gifts from Rohm & Haas Co. All chemicals were purchased from Sigma Chemical Co. in the highest available purity and were used without further purification.

Adsorption. The beads (0.3 g) were wetted with ethanol prior to use. After ethanol removal by filtration and washing with distilled water, the carrier was washed with 10 mL of 5 mM ammonium bicarbonate at pH 7.8 (ABC buffer). The supernatant was removed and replaced with 30 mL of ABC buffer containing 30 mg CALB. The vials containing the carrier and lipase were shaken gently, and the adsorption process was followed by measuring the disappearance of enzyme from the supernatant using a BCA assay (Sigma-Aldrich). When the concentration of lipase in the supernatant remained constant with increased incubation time, the carrier was filtered, washed with ABC buffer, and dried over silica gel under reduced pressure for 1 day. The loading of CALB on the supports (mg CALB/g support) was calculated from the amount of enzyme in the combined supernatant and washing fractions. The loading is defined as the amount of CALB (mg) lost from the solution per unit of the total weight of support and the amount of enzyme.

Control of Water Content. CALB physically immobilized on macroporous poly(methyl methacrylate) (PMMA) resin was dried over P_2O_5 using a pump with a drying pistol (5 mmHg; overnight; room temperature) so as to achieve a water content in the range from 0.6% (w/w) to 1.9%. Biocatalyst water contents (wt %) were measured by using an Aqua star C 3000 titrator with Coulomat A and Coulomat C from EMscience. Biocatalyst water content was determined by stirring 50 mg of immobilized enzyme in Coulomat A within the Aqua star container and titrating against Coulomat C.

Enzyme-Catalyzed Ring-Opening Polymerization of ϵ-Caprolactone. The activities of immobilized CALB preparations were determined for ϵ-caprolactone (ϵ-CL) polymerizations. Reactions were monitored by in-situ ^{1}H NMR experiments with the NMR probe at 70 °C. ^{1}H NMR measurements were performed on a Bruker DPX 300 spectrometer. Chemical shifts in parts per million (ppm) for ^{1}H NMR spectra were referenced relative to tetramethylsilane (TMS, 0.00 ppm) as the internal reference. Into 5 mm NMR tubes were transferred ϵ-CL (0.06 mL) and toluene-d_8 (0.7 mL), and tubes were placed in an external bath set at 70 °C. Then, immobilized resins were added. The weight ratio of CALB to ϵ-CL was maintained at 1:100 for all ring-opening polymerization experiments. After every scan (around 5−8 min), NMR tubes were removed from the probe, shaken well to mix tube contents, and then inserted back in the probe for the next scan. This procedure was performed as rapidly as possible to avoid fluctuations in the reaction temperature.

Enzyme-Catalyzed Condensation of Adipic Acid and 1,8-Octanediol. Immobilized lipase (1%-by-weight CALB relative to the total weight monomer) was transferred into a 100 mL round-bottom flask containing adipic acid (2.92 g, 20.0 mmol), 1,8-octanediol (2.92 g, 20.0 mmol), and a magnetic stir bar. The reaction flask was then placed into a 90 °C oil bath on a magnetic stirrer (IKA

(22) van Roon, J. L.; Joerink, M.; Rijkers, M. P. W. M.; Tramper, J.; Schroe1n, C. G. P. H.; Beeftink, H. H. *Biotechnol. Prog.* **2003**, *19*, 1510−1518.
(23) Vertegel, A. A.; Siegel, R. W.; Dordick, J. S. *Langmuir* **2004**, *20*, 6800−6807.
(24) Blanco, R. M.; Terreros, P.; Fernandez-Perez, M.; Otero, C.; Diaz-Gonzalez, G. *J. Mol. Catal. B: Enzymatic* **2004**, *30*, 83−93.
(25) Fernandez-Lorente, G.; Fernandez-Lafuente, R.; Palomo, J. M.; Mateo, C.; Bastida, A.; Coca, J.; Haramboure, T.; Hernandez-Justiz, O. et al. *J. Mol. Catal. B: Enzymatic* **2001**, *11*, 649−656.
(26) Nakaoki, T.; Mei, Y.; Miller, L. M.; Kumar, A.; Kalra, B.; Miller, M. E.; Kirk, O.; Christensen, M.; Gross, R. A. *Ind. Biotechnol.* **2005**, *1*, 126−134,
(27) van Roon, J.; Beeftink, R.; Schroën, K.; Tramper, H. *Curr. Opin. Biotechnol.* **2002**, *13*, 398−405.
(28) Mei, Y.; Miller, L.; Gao, W.; Gross, R. *Biomacromolecules* **2003**, *4*, 70−74.

Table 1. CALB Immobilization on MMA Resins of Differing Particle Size: Enzyme Loading, Fraction of Active Lipase, and Catalytic Activity

resin no.	sample name	avg pore diameter (Å)	particle size (μm)	surface area (m^2/g)	enzyme loading (% w/w, ±5%)	enzyme loading (mg/m^2, ±5%)	fraction active lipase (%, ±8%)	reaction constant ($k_{app,}$ min^{-1}, ±5.7%)	turnover frequency (s^{-1})[a]
1	Amberlite XAD-7HP	250	560−710	500	5.1	0.102	40.4	0.0012	3.0
2	Amberchrom CG-71C	250	120	500	5.2	0.104	44.2	0.0024	4.9
3	Amberchrom CG-71M	250	75	500	5.4	0.106	45.0	0.0033	5.6
4	Amberchrom CG-71S	250	35	500	5.7	0.114	43.0	0.0058	8.5

[a] Defined as number of ϵ-caprolactone molecules reacting per active site in 80 min in ring-opening polymerizations performed at 70 °C in toluene.

Werke, Rct Basic) at 300 rpm for 30 min to melt monomers. After 2 h, vacuum was applied (10 mm of Hg) to facilitate water removal. Aliquots of approximately 20 mg were removed at selected time intervals. Reactions were terminated by adding excess cold chloroform, stirring for 15 min, removing the immobilized enzyme by filtration, and washing beads 2 times with chloroform to extract remaining polymer. Molecular weight of reaction products was determined by gel permeation chromatography (GPC) using a Waters HPLC system equipped with model 510 pump, Waters model 717 autosampler, model 410 refractive index detector, and Viscotek Corporation model T-50/T-60 detector with 500, 10^3, 10^4, and 10^5 Å Ultrastyragel columns in series. Trisec GPC software version 3 was used for calculations. THF was used as eluant at 1.0 mL/min and the injections were 100 μL. Molecular weights were determined from a conventional calibration curve generated by narrow molecular weight polystyrene standards obtained from Aldrich Chemical Co.

Imaging of Protein Distribution by Infrared Microscopy. The method here is identical to that described elsewhere.[28] In summary, infrared microscopy was employed to determine the distribution of CALB within beads. Beads were embedded in paraffin wax, and the blocks were sectioned at a thickness of 8 μm using a stainless steel blade. Sections were coated on BaF_2 disks and placed in a standard FTIR slide mount for data collection. Spectra were collected in the transmission mode from 4000 to 750 cm^{-1}. The peak areas of *A* (1610−1670 cm^{-1}) and *B* (1700−1760 cm^{-1}) are proportional to amounts of CALB and PMMA, respectively. Enzyme concentration was calculated from the peak area corresponding to CALB divided by that of each resin. A Magna 860 FTIR spectrometer (Thermo Nicolet) and Synchrotron light from Beamline U10B at the National Synchrotron Light Source (Brookhaven National Laboratory) was used for small beads (35 and 75 μm), while a Spotlight FTIR spectrometer (Perkin-Elmer) was used for larger beads (120 and 560−710 μm).

Synthesis of Inhibitor Methyl *p*-Nitrophenyl *n*-Hexyl Phosphate (MNPHP). The method used was adapted from that described previously.[29,30,31] To a solution of *n*-hexylphosphonic dichloride (3.2 g, 15 mmol) in 100 mL dry dichloroethane was added a solution consisting of methanol (12 mmol, 0.36 g) and *N*-methylimidazole (26 mmol, 2.1 g) in 100 mL of dichloroethane at 4 °C. The reaction was slowly warmed to 25 °C with stirring for 1.5 h. Subsequently, a mixture of *p*-nitrophenol (22.5 mmol, 3.13 g) and *N*-methylimmidazole (26 mmol, 2.1 g) in 30 mL of dichloroethane was added, and the reaction was maintained at room temperature for 16 h. The reaction mixture was then diluted with 250 mL of dichloroethane, washed in a separatory funnel by extraction with 2% HCl (2 × 200 mL), 10% sodium bicarbonate (2 × 200 mL), and water (2 × 50 mL), respectively. The organic phase was dried over sodium sulfate, and the solvent was removed under reduced pressure. The reaction product (0.48 g, 29% yield) was obtained by flash chromatography (silica gel) using CH_3CHCl_2/EtOAc (9:1) as elution solvent.

^{1}H NMR (300 MHz, $CDCl_3$) 0.91 (t, 3H, CH_2-CH_3), 1.29−1.33 (m, 4H), 1.43 (qu, 2H), 1.68−1.73 (m, 2H), 1.90−2.00 (m, 2H, $-PCH_2-$), 3.84 (d, J_H-P =11.2 Hz, 3H, $-O-CH_3$), 7.4 (d, J = 8.7 Hz, 2H, Ph (2,6)), 8.25 (d, J = 8.8 Hz, 2H, Ph (3,5)).

Active-Site Titration of Immobilized Lipase in Hexane. The method used was adapted from that described previously.[31] A stock solution of methyl *p*-nitrophenyl *n*-hexyl phosphate (MNPHP) was prepared by adding MNPHP (12.04 mg, 40 mmol) to 4 mL of dry diethyl ether. The MNPHP diethyl ether solution (40 μL) was added to dry hexane (1.96 mL). Immobilized enzyme was preequilibrated in desiccators with saturated KCL solution to the desired water activity (a_w = 0.75) at room-temperature overnight. In a sealed vial, 2 mL of MNPHP diethyl ether/hexane solution was added to the immobilized enzyme (50 mg). After a 16 h reaction at 25 °C with shaking, the solvent was removed by vacuum. The mixture was then washed twice with 2 mL of acetonitrile (AcCN), and the concentration of *p*-nitrophenol was determined by LC-MS. The Waters LC-MS was equipped with a Waters Alliance 2795 system (Milford, MA), Waters 2996 UV detector (Milford, MA) set at 315 nm and a reversed-phase column (PLRP-S, Polymer Labs, pore size 1000 Å, particle size 8 μm, dimension 250 × 4.6 mm). Analyses were performed at room temperature with water/acetonitrile (40:60) mobile phase at a flow rate of 1 mL/min. The LC system, equipped with the electrospray source, was used with nitrogen as the desolvation gas. The ESI voltage supplied to a stainless steel needle was 3500 V, and the cone voltage was set at 10 V. The desolvation chamber was held at 200 °C, and the source block temperature was set at 100 °C. The mass spectrometric measurement was conducted by scanning the first quadrupole mass analyzer. Afterward, the carriers were washed twice with 5 mL of AcCN, dried by vacuum, and assayed for enzyme activity via ring-opening polymerization of ϵ-caprolactone for half an hour (see above).

Results and Discussion

A series of methyl methacrylate resins (see Table 1) with identical average pore diameter (250 Å) and surface area (500 m^2/g) but with varied particle size (35 to 560−710 μm) were studied to assess how particle size effects CALB adsorption and activity for lactone ring-opening and condensation polymerizations.

CALB Adsorption on Particles. The shape of an adsorption isotherm provides information on the rate of adsorption as well as the maximum equilibrium loading of the adsorbed substance. Figure 1 shows that CALB adsorption onto MMA beads was strongly dependent on bead size. Adsorption occurred more rapidly for smaller beads. All resins showed typical saturation behavior, and the saturation time increased as bead particle size increased. Saturation occurred in less than 30 s for sample 4 (AmberchromCG-71S, 35 μm) compared to 48 h for sample 1 (AmberchromCG-71S, 560−710 μm). The dependence of adsorption rate on particle size is due to the pore size that is limiting protein transport to the inside of particles. In other words, the small size of pores slows protein diffusion into beads so that smaller beads more rapidly were saturated in protein. Adsorption yields for all bead sizes studied were about 55% when the initial enzyme and bead concentrations used for immobilization were 1 and 10 mg/mL, respectively. As long as sufficient time is given to reach the maximum equilibrium loading value, total enzyme

(29) Oskolkova, O. V.; Hermetter, A. *Biochim. Biophys. Acta* **2002**, *1597*, 60−66.
(30) Stadler, P.; Zandonella, G.; Haalck, L.; Spener, F.; Hermetter, A.; Paltauf, F. *Biochim. Biophys. Acta* **1996**, *1304*, 229−244.
(31) Rotticci, D.; Norin, T.; Hult, K.; Martinelle, M. *Biochim. Biophys. Acta* **2000**, *1483*, 132−140.

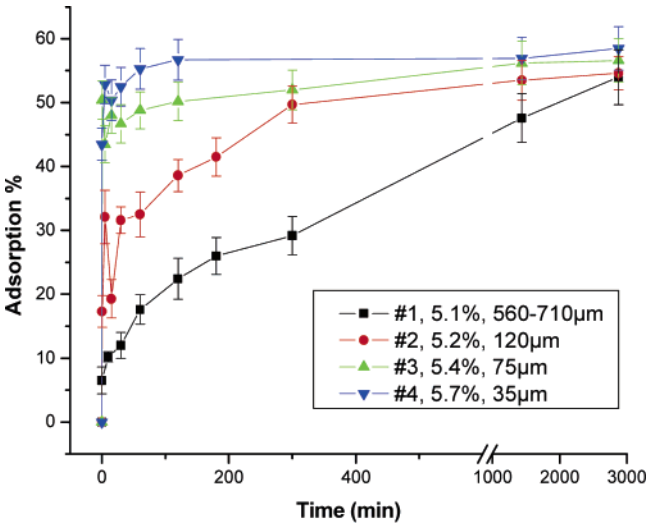

Figure 1. Adsorption isotherms of CALB onto resins that differ in particle size.

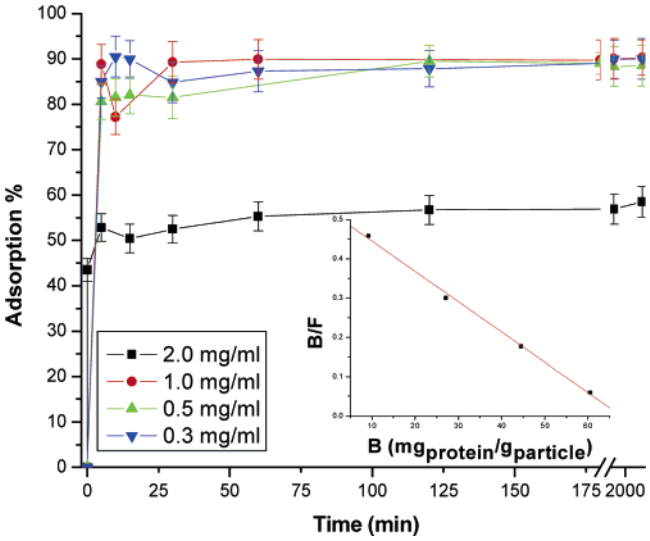

Figure 2. Adsorption isotherms of CALB on Amberchrom CG-71S with 35 μm diameter using CALB solutions that differ in concentration. Inset shows linearization of the adsorption isotherm by using the Scatchard analysis to determine the limiting adsorption of CALB. *B* is weight (mg) of protein molecules bound to 1 g of resin beads. *F* is concentration of native enzyme in μg/mL.

loading is not controlled by the particle size. Thus, similar numbers of adsorption sites are available within resins which correspond to identical values of surface area through the broad range of bead particle sizes studied. In a previous study by Jeroen L. van Roon et al.,[22] loading of penicillin-G acylase (Assemblase) onto MMA beads was inversely related to with bead size. In light of the results herein, lower loading for larger size beads may be explained by insufficient incubation time so that saturation was not reached.

Figure 2 shows that, when different enzyme concentrations were used for adsorption onto sample 4 (AmberchromCG-71S, 35 μm), loading saturation was achieved in 30 min. Enzyme loading was increased by increasing the enzyme concentration for immobilization until the limiting adsorption is reached. That led to a decrease in the adsorption yield from 90% to 60%. The Scatchard analysis was used to determine the limiting adsorption of CALB onto 35 μm diameter Amberchrom CG-71S. In this method, linearization of the adsorption isotherm is achieved by using eq 1:

$$B/F = B_{lim}/C - B/C \quad (1)$$

where *B* is weight (mg) of protein molecules bound to 1 g of resin beads, *F* is concentration of native enzyme in μg/mL, B_{lim} is the limiting adsorption given as the number of available adsorption sites per resin particle, and *C* is the constant for dissociation of protein from the surface. By this analysis, B_{lim} for the 35 μm macroporous particles is 71.8 mg/g (0.144 mg/m^2) which is much lower than 2.74 mg/m^2 that, assuming CALB exists on the surface in its native state, is the density of enzyme needed to form a monolayer and fully cover the support surface. Therefore, it appears that CALB molecules are isolated from one another along the surface although some fraction of these molecules may be CALB aggregates. The value of C for this resin-enzyme system is 3.9 μM which shows that CALB has a high affinity for the resin surface.

Active Lipase Fraction. MNPHP is a well-known irreversible inhibitor of lipases that is highly specific for reaction with active-site serine residues. Thus, MNPHP was selected as the inhibitor to determine, by titration, the fraction of catalytic sites that are accessible and active. Since we are concerned with CALB activity in organic media, inhibition was studied in heptane. LC-MS was used to determine the release of *p*-nitrophenol (*p*NP) which corresponds with accessible active sites. To ensure that adsorption of *p*NP by resins was taken into consideration, *p*NP concentration was corrected as follows. A fixed quantity of enzyme-free resin was incubated overnight in acetonitrile with different concentrations of *p*NP. Standard curves of *p*NP adsorption by each resin as a function of *p*NP concentration were constructed from LC-MS measurements. MNPHP-inhibited immobilized enzymes were used for ϵ-caprolactone ring-opening polymerizations in toluene (70 °C). No conversion of monomer was observed in 30 min. Hence, MNPHP titration resulted in complete inhibition of CALB activity.

By inspecting fraction of active site values in Table 1 we conclude that CALB adsorption onto resins 1−4 results in >50% deactivation of immobilized CALB molecules. This may be due to enzyme denaturation and/or inaccessibility of active sites upon CALB adsorption to MMA support surfaces. At enzyme-loadings of 5−6%, the fraction of active sites for immobilized CALB ranged from 40 to 45%. Thus, the fraction of active CALB molecules was independent of resin size for supports that ranged from about 600 to 35 μm. This fraction of active immobilized lipase molecules is very close to results determined by titration with MNPHP of *C. antarctica* lipase A (CALA) and *Humicola lanuginosa* lipase (HLL) immobilized on Accurel in heptane.[31]

Enzyme loading on 35 μm AmberchromCG-71S (300 mg) was varied from 0.92 to 5.7% (w/w) by changing the enzyme concentration from 0.2 to 1 mg/mL during incubations. A substantial and regular change in the fraction of CALB active sites was observed as a function of CALB loading. MMA 35 μm resins with 0.92, 2.64, 4.26, and 5.70% w/w CALB have 33.1, 38.4, 43.0, and 45.9% of CALB molecules whose catalytic sites are active (see Table 2). Hence, by increasing enzyme loading on the resin, the fraction of active sites increased. This may be due to changes in the fraction of aggregated CALB molecules along surfaces. It is likely that aggregated CALB molecules on MMA will have different activities than CALB molecules that are isolated from one another. Possibly, the confirmation adopted by CALB aggregates leads toward a larger fraction of active sites. Alternatively, closer average distances between CALB molecules and resulting protein−protein interactions may cause reorientation of CALB molecules on surface so that their active sites are more accessible to substrates. In a related study, G. Belfort et al. reported that, as adsorption proceeds, ribonuclease

Table 2. CALB Immobilization on Amberchrom CG-71S 35 μm Diameter Beads: Effect of CALB Loading on the Fraction of Active Lipase and Catalyst Activity[a]

entry	CALB/resin (w/w mg/g)	CALB concd (mg/mL)	CALB loading (% w/w, ±5%)	CALB loading (mg/m^2, ±5%)	fraction active CALB (%, ±8%)	reaction constant (min^{-1}, ±5.7%)	turnover frequency (s^{-1})[b]
1	10	0.2	0.9	0.053	30.5	nd[c]	nd
2	30	0.3	2.6	0.085	33.1	0.0008	0.91
3	50	0.5	4.3	0.114	38.4	0.0024	4.9
4	100	1	5.7	0.168	43.0	0.0057	8.5

[a] Protein solution (15 mL) and 300 mg resins were used for immobilization. For other immobilizations, 30 mL of protein solution and 300 mg resins were used. [b] Defined as moles of ϵ-caprolactone reacting per mole of CALB active sites in 80 min. [c] Not determined (nd) since sufficient resolution in NMR experiments was not achieved to provide meaningful data.

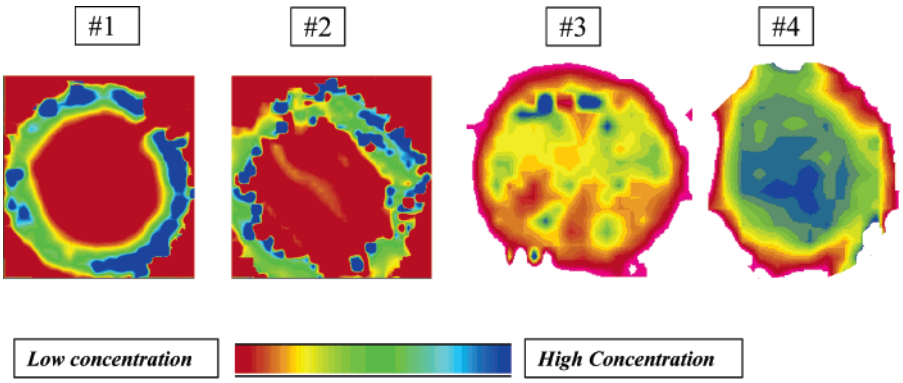

Figure 3. Infrared microspectroscopy images to analyze CALB distribution within a series of MMA resins that differ in particle size (1 is Amberlite XAD-7HP, 600 μm diameter; 2 is Amberlite XAD-71C, 120 μm diameter; 3 is Amberchrom CG-71M, 75 μm diameter; 4 is Amberchrom CG-71S, 35 μm diameter).

A (RNase A) molecules slowly reorient until they eventually lie end-on with their largest axis perpendicular to the surface and their active site partially exposed to the free solution.[32] These results enable kinetic studies to be performed based on the concentration of active lipase instead of total enzyme concentration.[33−37] Work is in progress by our laboratory using well-defined flat film surfaces where it is possible to better quantitate protein aggregation, determine protein orientation, and correlate these factors with protein activity.

CALB Distribution within Immobilized Support. Figure 3 displays infrared images of protein distribution for CALB on MMA resins that differ in particles size. CALB forms a protein loading front for sample 1, Amberlite XAD-7HP, and sample 2, Amberlite XAD-71C, with particle sizes 560−710 and 120 μm, respectively. The thickness of protein loading fronts for these beads with particle sizes 560−710 and 120 μm is 100 μm and 40 μm, respectively. Thus, approximately 50% and 30%, respectively, of the internal bead volumes do not contain CALB. CALB penetrates to the inside of sample 3, AmberchromCG-71M (75 μm). For sample 4, the infrared image shows that CALB is distributed throughout this polymer resin. Previously, we reported that narrow polydispersity polystyrene with M_n 46 kD readily diffuses throughout Novozyme 435,[28] which consists of CALB physically immobilized within a macroporous resin of PMMA (Lewatit VP OC 1600, average particle and pore size 315−1000 and 150 μm, respectively). Thus, for larger beads where CALB forms a protein loading front, substrates and products diffuse in and out of bead regions that lack the immobilized enzyme which leads to nonoptimal catalyst performance.

Immobilized CALB Activity. The activity of CALB immobilized on resins 1−4 (see Table 1) was assessed by ϵ-CL ring-opening polymerizations. All immobilized resins have similar CALB loading (5.1−5.7%-by-wt) and water content (1.4−1.9%). As shown previously,[33] different chemical shifts are observed for methylene protons (−OCH_2−) of ϵ-CL monomer, PCL internal repeat units, and chain terminal −CH_2−OH moieties. Hence, by in situ NMR monitoring, monomer conversion and polymer number average molecular weight (M_n) were determined.

As Figure 4 illustrates, the polymerization rate strongly depends on the matrix particle size used for CALB immobilization. For example, at about 80 min reaction time, as the particle size decreased from 560−710 to 120, 75, and 35 μm, the turnover frequency (TOF) for ϵ-CL increased from 3.0 to 4.9, 5.6, and 8.5. Correspondingly, ϵ-CL %-conversion increased from 20 to 36, 42, and 61%, respectively. Each experiment was repeated at least three times, and variability was assessed by comparison of apparent rate constant values, (k_{app}, min^{-1}). Variability in k_{app} values was ±5.7% which validated the significance of data reported herein. Error bars were not included for conversion values in Figure 4 since, by using in situ NMR to determine %-ϵ-CL conversion, times at which conversion values were measured between experimental runs varied slightly.

Plots of log([M]$_0$/[M]$_t$) versus time and M_n versus %-ϵ-CL conversion were constructed and are displayed in Figure 5. All plots in Figure 5a demonstrate a linear relationship with correlation coefficients of >0.99. Thus, regardless of the matrix particle size, monomer conversion followed a first-order rate law and termination reactions did not occur.[34] Similar behavior was observed for ϵ-CL ring-opening polymerizations catalyzed by Novozym 435 where CALB is immobilized on Lewatit.[34−37]

(32) Lee, C.-S.; Belfort, G. *Proc. Natl. Acad. Sci.* **1989**, *86*, 8392−8396.
(33) Mei, Y.; Kumar, A.; Gross, R. A. *Macromolecules* **2002**, *35*, 5444−5448.
(34) Deng, F.; Gross, R. A. *Int. J. Biol. Macromo.* **1992**, *25*, 153−159.
(35) Henderson, L. A.; Svirkin, Y. Y.; Gross, R. A.; Kaplan, D. L.; Swift, G. *Macromolecules* **1996**, *29*, 7759−7766.
(36) Matsumoto, M.; Odachi, D.; Kondo, K. *Biochem. Eng. J.* **1999**, *4*, 73−76.
(37) Mei, Y.; Kumar, A.; Gross, R. *Macromolecules* **2003**, *36*, 5530−5536.

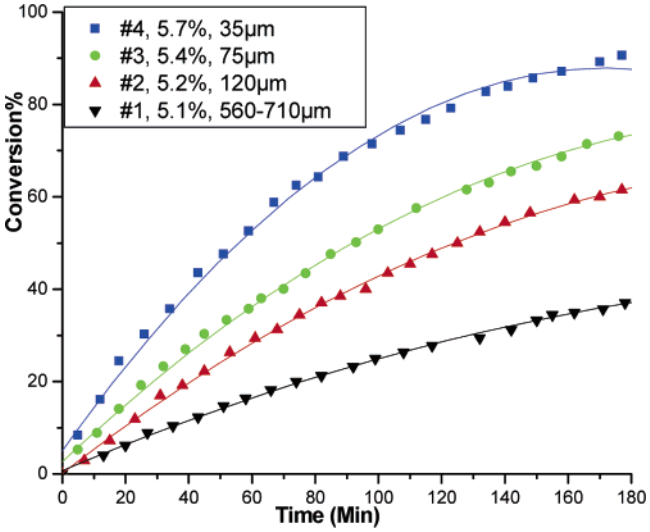

Figure 4. Effect of immobilized CALB particle size (given in micrometters, see legend box in plot) on the time course of ϵ-caprolactone ring-opening polymerizations performed at 70 °C in toluene.

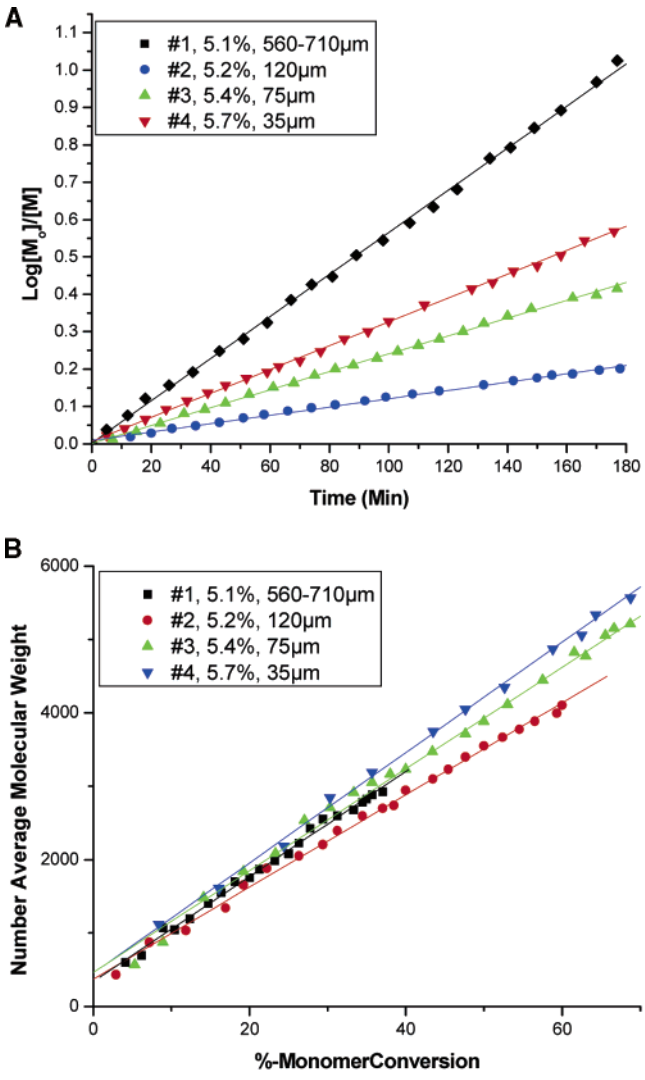

Figure 5. Immobilized CALB catalysis of ϵ-caprolactone ring-opening polymerizations performed at 70 °C in toluene: (a) semilogarithmic plot, (b) M_n versus percent monomer conversion.

The activity of immobilized CALB catalysts was quantified by determining reaction kinetic constants (k_{app}) by taking the slope of log([M_0]/[M]) versus time plots. As the particle size decreased from 560−710 to 120, 75, and 35 μm, k_{app} increased from 0.0012 to 0.0024, 0.0033, and 0.0057 (min^{-1}), respectively. Since the fraction of active lipase is not influenced by particle size (see Table 1), increased catalytic activity when using resins of smaller size is due to a higher frequency of collisions between substrates and CALB. Correspondingly, by decreasing the resin particle size, constraints for substrate and product diffusion to and from immobilized enzyme are reduced. Only CALB immobilized on resin 4 with 35 μm particles showed a nearly uniform distribution of enzyme throughout beads (see above). CALB immobilized on resins 1 and 2 showed large regions within beads with little or no CALB so that diffusion of substrate and product to enzyme-deficient regions within beads is nonproductive with respect to polymer forming reactions. Similarly, Nakaoki et al. reported that physically adsorbed CALB catalysts showed higher activity for ϵ-CL ring-opening polymerizations when CALB was distributed throughout carriers.[26]

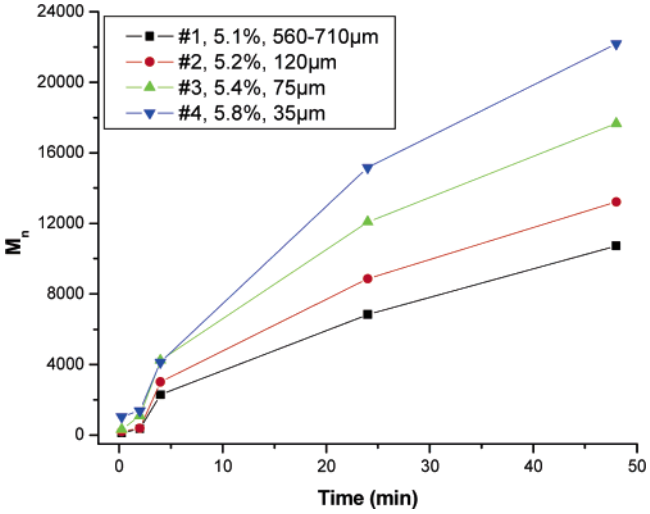

Figure 6. Immobilized CALB catalysis of adipic acid/1,8-octanediol condensation polymerization at 90 °C in bulk.

Plots of M_n versus percent ϵ-CL conversion were constructed and are displayed in Figure 5b. All plots in Figure 5b are linear with correlation coefficients of >0.99. Thus, regardless of the matrix particle size, chain transfer to monomer was not observed and the polymerization occurs by a chain-growth mechanism where ϵ-CL units are ring-opened by propagating chain ends.[35] Since water content in reactions is similar, the total number of propagating chains should also be similar for ϵ-CL polymerization catalyzed by CALB immobilized on resins 1−4. Hence, this explains that M_n at fixed monomer conversion values changed little as a function of resin size.

The activity of CALB immobilized on resins 1−4 was also assessed by condensation polymerizations of adipic acid and 1,8-octanediol (Figure 6). As above, all immobilized resins have similar CALB loading (5.1−5.7%-by-wt) and water content (1.4−1.9%). As the particle size decreased from 560−710 to 120, 75 and 35 μm, the molecular weight at 24 h increased from 6.8k to 8.8k, 12.1k, and 15.2k, respectively. These results are in excellent agreement with those for ϵ-CL ring-opening polymerizations (see above). As above, increased chain growth during poly(octanyl adipate) synthesis is explained by increased diffusion of substrates and products to and from immobilized enzyme when using resins of smaller size.

The polymerization rate strongly depends on the enzyme loading (Figure 7). At about 80 min reaction time, as enzyme loading on resin 4 increased from 2.6 to 4.3 and 5.7%, TOF of

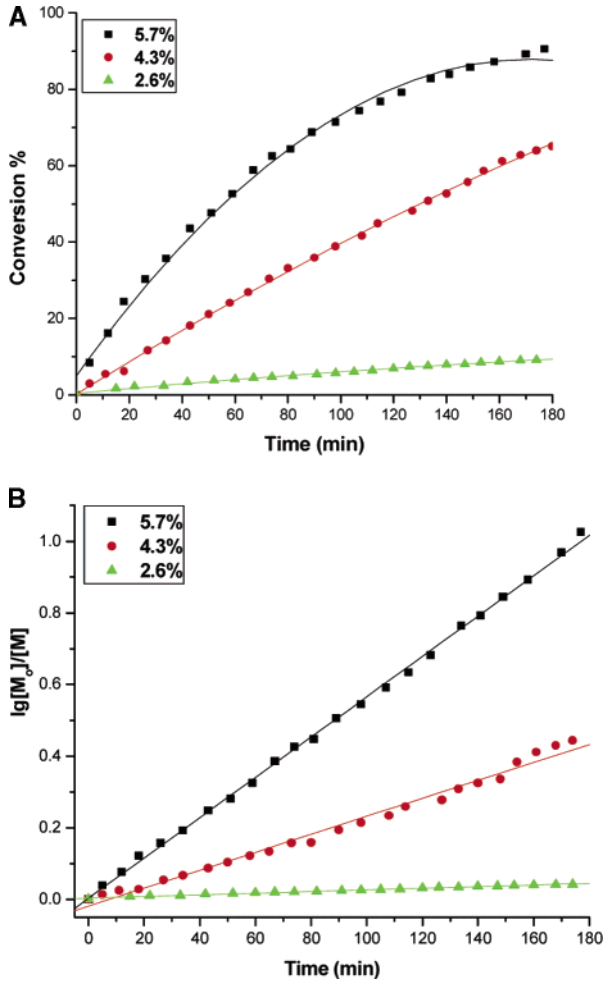

Figure 7. Effect of the CALB loading (see legend box in plots) onto Amberchrom CG-71S with 35 μm bead diameter on the time course (a) and semilogarithmic plots (b) for ϵ-caprolactone ring-opening polymerizations at 70 °C in toluene.

ϵ-CL molecules increased from 0.9 to 4.9 and 8.5 in 80 min, respectively. Correspondingly, ϵ-CL %-conversion increased from 5 to 31 and 61%, respectively. Catalytic efficiency of immobilized CALB with different enzyme loadings was analyzed by determining apparent kinetic constants (k_{app}) by taking the slope of log([M_0]/[M]) versus time plots (Figure 7, Table 2). As the enzyme loading on resin 4 increased from 2.6 to 4.3 and 5.7%, k_{app} increased from 0008 to 0.0024 and 0.0057 min^{-1}, respectively. Similar results were observed that by increasing the density of CALB per unit surface area of resin, such as with QDM 2-3-4 and Accurel, CALB activity increased for CL polymerizations.[26] This nonlinear relationship between enzyme concentration and reaction rate is consistent with an increased fraction of active CALB molecules, from 30.5 to 43.0%, by increasing enzyme loading from 0.9 to 5.7 (see above). Furthermore, increase in enzyme loading on resin 4 results in a more uniform distribution of enzyme throughout beads which was shown previously to be beneficial to catalyst activity.[26] Additional work will be needed to define whether rate equations for ϵ-CL polymerizations change as a function of enzyme environment within macroporous resins.

Summary of Results

C. antarctica lipase B (CALB) was immobilized by physical adsorption onto cross-linked poly(methyl methacrylate) resins with high yield. Immobilized CALB displayed high activity and similar mechanism in chain propagation toward ring-opening polymerization of ϵ-CL in toluene. Decrease of the resin diameter did not influence the fraction of active CALB molecules. However, by decreasing resin diameter at nearly constant protein loading, increases in (i) CALB adsorption onto resins, (ii) rate of ϵ-CL conversion in ring-opening polymerization, and (iii) growth of poly(octanyl-adipate) chains were observed. These results were explained by decrease in diffusional constraints with smaller diameter resins. By increasing enzyme loading, increases in both the fraction of active CALB molecules and catalyst efficiency for ϵ-CL ring-opening polymerization were observed. A nonuniform distribution with most enzyme present in the outer region of particles was found by IR microspectroscopy with 560−710 and 120 μm diameter resins. In contrast, as the resin particle size was decreased, the protein distribution became increasingly uniform throughout resins. These results showed the benefits of systematic investigations of immobilization parameters to achieve enhanced enzyme−catalyst activities. However, much work remains to understand on a molecular level how, for example, changes in enzyme loading influences the fraction of active lipase. Details of enzyme conformation and orientation as a function of surface chemistry and morphology on model systems taken together with better control of surface chemistry and morphology when designing macroporous resins will lead to important catalyst improvement.

Acknowledgment. The authors thank the NSF and industrial members (BASF, Novozymes, Johnson & Johnson, Rohm and Haas, Genencor, Estée Lauder, DNA 2.0, W.R. Grace, Grain Processing Corporation, and DeGussa) of the NSF-Industry/University Cooperative Research Center (NSF I/UCRC) for Biocatalysis and Bioprocessing of Macromolecules at Polytechnic University for their financial support, intellectual input, and encouragement during the course of this research.

LA062258U